Pathology (June 2024) **56(4)**, pp. 493–503

ANATOMICAL PATHOLOGY

Non-coding RNA and gene expression analyses of papillary renal neoplasm with reverse polarity (PRNRP) reveal distinct pathological mechanisms from other renal neoplasms

Stéphane Nemours[1], María Armesto[1], María Arestín[1], Claudia Manini[2,3], Doriana Giustetto[4], Maris Sperga[5], Kristyna Pivovarcikova[6], Delia Pérez-Montiel[7], Ondrej Hes[6], Michal Michal[6,8], José I. López[9], Charles H. Lawrie[1,10,11,12]

[1]*Biogipuzkoa Health Research Institute, Oncology Area, Molecular Oncology Group, San Sebastian, Spain;* [2]*Department of Pathology, San Giovanni Bosco Hospital, ASL Città di Torino, Turin, Italy;* [3]*Department of Sciences of Public Health and Pediatrics, University of Turin, Italy;* [4]*Department of Pathology, Maria Victoria Hospital, ASL Città di Torino, Turin, Italy;* [5]*Department of Pathology, Stradin's University, Riga, Latvia;* [6]*Department of Pathology, Faculty of Medicine in Pilsen, Charles University, Pilsen, Czech Republic;* [7]*Department of Pathology, National Institute of Cancer, Mexico City, Mexico;* [8]*Bioptical Laboratory Ltd, Pilsen, Czech Republic;* [9]*Biocruces-Bizkaia Health Research Institute, Barakaldo, Spain;* [10]*IKERBASQUE, Basque Foundation for Science, Bilbao, Spain;* [11]*Sino-Swiss Institute of Advanced Technology (SSIAT), University of Shanghai, Shanghai, China;* [12]*Radcliffe Department of Medicine, University of Oxford, Oxford, UK*

Summary

Papillary renal neoplasm with reversed polarity (PRNRP) is a recently described rare renal neoplasm. Traditionally, it was considered a variant of papillary renal cell carcinoma (PRCC). However, several studies reported significant differences between PRNRP and PRCC in terms of clinical, morphological, immunohistochemical and molecular features. Nonetheless, PRNRP remains a poorly understood entity. We used microarray analysis to elucidate the non-coding RNA (ncRNA) and gene expression profiles of 10 PRNRP cases and compared them with other renal neoplasms. Unsupervised cluster analysis showed that PRNRP had distinct expression profiles from either clear cell renal cell carcinoma (ccRCC) or PRCC cases at the level of ncRNA but were less distinct at the level of gene expression. An integrated omic approach determined miRNA:gene interactions that distinguished PRNRP from PRCC and we validated 10 differentially expressed miRNAs and six genes by quantitative RT-PCR. We found that levels of the miRNAs, *miR-148a, miR-375* and *miR-429*, were up-regulated in PRNRP cases compared to ccRCC and PRCC. miRNA target genes, including KRAS and VEGFA oncogenes, and CXCL8, which regulates VEGFA, were also differentially expressed between renal neoplasms. Gene set enrichment analysis (GSEA) determined different activation of metabolic pathways between PRNRP and PRCC cases. Overall, this study is by far the largest molecular study of PRNRP cases and the first to investigate either ncRNA expression or their gene expression by microarray assays.

Key words: Renal cancer; miRNA; transcriptome; pathway analysis; papillary renal neoplasm with reversed polarity.

Received 9 June, revised 25 October, accepted 14 November 2023
Available online 7 February 2024

INTRODUCTION

Renal carcinomas are amongst the most common neoplasms in the Western world, representing about 3% of all malignant tumours in adults.[1] Therefore, their clinical management represents a major concern for health services worldwide.[2] Between 80% and 90% of renal carcinomas are either clear cell renal cell carcinoma (ccRCC; 70–80%) or papillary RCC (PRCC; 10–15%) although there are at least 20 other distinct forms of RCC recognised by the World Health Organization (WHO).[3–8] Emerging or provisional entities have been considered as variants of PRCC,[9] including papillary renal neoplasm with reversed polarity (PRNRP).[10]

PRNRP is an indolent tumour (without reported mortality) with papillary or tubulopapillary architecture and a single layer of eosinophilic cells with finely granular cytoplasm and apically located round nuclei with inconspicuous nucleoli.[10] To date, there have been ~150 cases of PRNRPs reported in the literature, however, studies have focused on the histomorphological features and less frequently on associated genetic abnormalities.[11–18] For example, GATA-3 and L1CAM positivity along with the presence of *KRAS* mutations (in 60–70% of PRNRP cases) are frequently associated with PRNRP and have been used to distinguish it from PRCC.[19–22] However, there are very few studies considering the molecular basis of PRNRP, and none to date that have considered the role that non-coding RNAs (ncRNA) such as microRNAs (miRNAs) could play in this disease.

DOI: https://doi.org/10.1016/j.pathol.2023.11.013

Various studies, including ours, have shown that different renal neoplasms have differing miRNA profiles that play important roles in the molecular pathogenesis of the respective diseases.[23,24] The aim of this study was to compare the miRNA (and other ncRNAs) expression of PRNRP with PRCC (and ccRCC) to distinguish the two renal neoplasms with potentially confounding diagnosis.

MATERIALS AND METHODS

Patient selection and patient material

Ten PRNRP cases analysed in this study were retrieved retrospectively from the archives of the Department of Pathology, Cruces University Hospital, University of the Basque Country (UPV/EHU); the Department of Pathology, Faculty of Medicine in Pilsen, Charles University, Pilsen, Czech Republic; the Department of Pathology, San Giovanni Bosco Hospital, Turin, Italy; and the Department of Pathology, Stradin's University, Riga, Latvia. Cases were only considered for this study after fulfilment of strict inclusive histological and immunohistochemical criteria.[10,11] For comparison, we selected a further 49 cases of renal carcinoma, 12 ccRCC cases and 20 cases of PRCC (formally type 1) and 22 renal tissue samples from non-neoplastic nephrectomies as previously described,[23] as well as a further 17 ccRCC cases (not yet published). The clinical details of the PRNRP cases can be found in Table 1. All PRNRP patients were alive and well at last follow-up, without any notable progression in renal-related pathologies. All patients consented to the use of their biopsies for research purposes by signing a consent form. This study complies with current Spanish and European Union laws and conforms to the principles of the Declaration of Helsinki.

Immunohistochemical analyses

Immunohistochemistry was performed using the Benchmark Ventana system (Roche, Switzerland). Antibodies against CK7 (790-4462, ready-to-use; Roche, Ventana, USA), GATA-3 (760-4897, ready-to-use; Roche, Ventana), racemase (790-6011, ready-to-use; Roche, Ventana), L1CAM (L4543, dilution 1:100; Sigma-Aldrich, USA) and Vimentin (790-2917, ready-to-use; Roche, Ventana) were used. Normal renal tissue adjacent to the neoplasm was used in every case as an internal negative control.

RNA purification and microarray analysis

Total RNA was extracted from formalin-fixed, paraffin-embedded (FFPE) biopsy material using the Recover All kit from Ambion (LifeTechnologies, UK). We used 2 µg of total RNA for Affymetrix Genechip miRNA v.4.0 microarrays, and 200 ng of DNAse treated RNA for Clariom D human microarrays to measure ncRNA and gene expression, respectively. RNA was labelled and hybridised to microarrays in accordance with the manufacturer's instructions (Affymetrix, USA). For this study we carried out both ncRNA and gene microarray analyses for all PRNRP samples (n=10) and gene array analysis for seven PRCC cases. The remainder of the microarray data came from previously published studies,[23] or for 17 ccRCC cases, from a study not yet published. The raw intensity data (i.e., cel files) were imported and analysed within Transcriptome Analysis Console (TAC) software version 4.0.2 (Affymetrix, USA). Using this software, we identified differentially expressed miRNAs or genes on the basis of greater than two-fold up- or down-regulation along with Benjamini–Hochberg multiple corrected p values <0.05. All microarray data were Minimum Information About a Microarray Experiment (MIAME) compliant. Analyses were conducted in R[25] and figures were produced using the package ggplot2.[26] For gene expression analysis, coding genes were classified as probes and filtered using the group variable 'coding' or 'multiple complex', before removing non-annotated genes that only had a numerical Ace view description. Raw data were deposited in the GEO database (accession numbers GSE255706 and GSE255707).

In order to identify differentially expressed genes that are likely to be regulated by miRNAs, a miRNA:target gene interaction network was produced as previously described.[27] Briefly, differentially expressed miRNAs and genes were mapped to a database of experimentally validated interactions (n=10,755) obtained from the miRTarBase dataset consisting of 3502 genes and miRNAs,[28] and were visualised using Cytoscape software (v3.9.1; National Institutes of Health, USA).[29]

Table 1 Clinicopathological characteristics of papillary renal neoplasm with reverse polarity cases included in this study

Case no.	Age, years	Sex	Procedure	Size, cm	P-stage	Capsule	Cystic	NG	CK7	Racemase	L1CAM	GATA3	Vimentin	*KRAS*	Follow-up, months	Update
1	75	F	Total nephrectomy	4	pT1b	N	N	1	+	–	+	+	–	p.G12X	120	Alive
2	61	M	Tumourectomy	1.3	pT1a	N	Y	1	+	+	+	+	–	p.G12X	4	Alive
3	70	M	Tumourectomy	1.8	pT1a	N	Y	1	+	f	+	+	–	p.G12X	1	Alive
4	75	F	Total nephrectomy	4	pT1a	Y	Y	1	+	+	NP	+	–	WT	7	Alive
5	73	M	Tumourectomy	1.7	pT1a	N	N	1	+	+	+	+	–	p.G12X	173	Death/other causes
6	69	M	Tumourectomy	0.5	pT1a	N	N	1	+	+	+	+	–	p.G12X	7	Alive
7	59	F	Total nephrectomy	1.3	pT1a	Y	Y	1	+	+	NP	+	–	p.G12X	168	Death/other causes
8	80	F	Total nephrectomy	1	pT1a	Y	Y	1	+	+	+	+	–	WT		
9	79	F	Total nephrectomy	1.6	pT1a	N	Y	1	+	+	+	+	–	p.G12X	13	Alive
10	45	F	Total nephrectomy	4	pT1b	Y	Y	1	+	+	NP	+	–	WT		

–, negative; +, positive; F, female; f, focally positive; M, male; N, no; NG, WHO/ISUP nuclear grade; NP, not performed; Y, yes.

Gene set enrichment analysis (GSEA) was performed using GSEA software package (https://www.gsea-msigdb.org/gsea/index.jsp) as previously described.[30,31] Analyses were performed to identify pathways (gene sets) that were enriched in PRNRP relative to PRCC cases or enriched in ccRCC relative to PRNRP. GSEA statistical significance was assessed using GSEA software that calculated false discovery rate (FDR).

Quantitative RT-PCR

To measure levels of individual miRNAs by qRT-PCR, we used 450 ng of total RNA. The RNA was reverse transcribed using the TaqMan Megaplex miRNA pool A according to the manufacturer's instructions (Applied Biosystems, UK). Pre-amplification of the resulting reaction was performed using the PreAmp Master Mix combined with PreAmp primers pool A according to the manufacturer's instructions (Applied Biosystems). qPCR was carried out with individual TaqMan probes using a LightCycler 96 System machine (Roche, Switzerland).

To measure levels of genes by qRT-PCR, we used 500 ng of total RNA. The RNA was reverse transcribed using the SuperScript IV VILO Master Mix according to the manufacturer's instructions (Invitrogen, USA). Pre-amplification of the resulting reaction was carried out using the PreAmp Master Mix combined with a TaqMan primer pool (0.2X) according to the manufacturer's instructions. qPCR for target genes was carried out with the same conditions as described above for the miRNA quantification. The small nucleolar RNA (snoRNA) RNU48 was used as the reference for miRNA quantification as previously described,[32] and *B2M* was used as a control for gene expression. The mean Ct value of each triplicate was calculated by the ΔCt method (i.e., ΔCt=mean Ct of *RNU48/B2M* minus the mean Ct of miRNA/gene of interest). All qRT-PCR assays were carried out in technical triplicate and expression levels were compared using the Mann–Whitney independent t-test (GraphPad Prism v.8.0, Dotmatics, USA).

RESULTS

Clinicopathological description

All the PRNRP cases displayed the characteristic papillary architecture, eosinophilic cellular appearance and reversal (anti-basal) polarity nuclei as reported previously (Fig. 1).[10–12,16,18,19,21,22,33–36] All PRNRP cases were positive for CK7, GATA3 and L1CAM staining. Nine of 10 cases were positive (either diffusely or focally) for racemase, while vimentin was negative in all cases (Fig. 1, Table 1) consistent with previous findings.[10–12,16,18,19,21,22,33–36] Seven of 10 cases had the *KRAS* gene mutated in position p.G12X as previously published.[11–14,16,18,19,21,33–36]

ncRNA and gene expression analyses

Microarray analyses to determine non-coding RNA expression were performed on the 10 PRNRP cases along with data from five PRCC and 29 ccRCC cases. Unsupervised cluster analysis of expression of mature miRNA (Fig. 2A), pre-miRNA (Supplementary Fig. 1A, Appendix A), small nucleolar RNA and small Cajal body-specific RNA (Supplementary Fig. 1B, Appendix A) clustered the PRNRP cases distinctly from either ccRCC or PRCC. Using ANOVA analysis, we identified 319 differentially expressed mature miRNAs between PRNRP and PRCC cases (Fig. 2B; Supplementary Table 1, Appendix A); 185 miRNAs differentially expressed between PRNRP and ccRCC (Fig. 2C, Supplementary Table 2, Appendix A); and 279 miRNAs differentially expressed between PRCC and ccRCC (Supplementary Fig. 2 and Supplementary Table 3, Appendix A).

We also carried out gene expression analysis on the 10 PRNRP cases, which we compared with seven PRCC samples and 17 ccRCC cases. Unsupervised cluster analysis of gene expression showed a general clustering of the PRNRP cases, but not as distinct as that observed with ncRNA expression (Fig. 2D). We identified 601 differentially expressed genes between PRNRP and PRCC (Fig. 2E), 2425 genes differentially expressed between PRNRP and ccRCC (Fig. 2F), and 1702 genes differentially expressed between PRCC and ccRCC (Supplementary Fig. 3, Appendix A). The list of top 100 differentially expressed genes up- and down-regulated for each tumour comparison are reported in supplementary Tables 4–9 (Appendix A).

Next, in order to identify differentially expressed genes between tumour types that are regulated by miRNAs, we used a previously described approach,[27] whereby we mapped the differentially expressed miRNA and genes to a database containing experimentally validated miRNA-gene target interactions derived from the miRTarBase database.[28] Resulting networks were created and visualised using the Cytoscape software,[29] one comparing PRNRP and PRCC (Fig. 3), and another one comparing PRNRP and ccRCC cases (Supplementary Fig. 4, Appendix A). For the network between PRNRP and PRCC, we identified 14 miRNAs that targeted 30 different genes with a total of 43 miRNA:target gene interactions (Table 2), and between PRNRP and ccRCC 17 miRNAs that targeted 33 genes in a total of 54 miRNA:target gene interactions (Supplementary Table 10, Appendix A). We observed that *miR-200a*, *miR-200c* and *miR-429*, members of the 200 family, *miR-155* and *miR-210* were present in both networks as were the target genes *KRAS*, *VEGFA*, *STAT3*, *ISCU*, *CXCL8* and *SERPINE1*.

qRT-PCR validation of miRNAs and genes

Based on the miRNA:gene interaction networks as well as literature searches, we selected ten miRNAs and six genes for further analysis and measured their expression by qRT-PCR in 10 PRNRP, 20 ccRCC and 20 PRCC cases along with 22 healthy control samples. Consistent with the array data, levels of *miR-155* and *miR-210* were lower in PRNRP and control tissues compared with ccRCC or PRCC cases (Fig. 4A,B, respectively) and levels of *miR-193b-3p* were down-regulated in PRNRP compared to ccRCC cases (Fig. 4C), but not PRCC or controls. Levels of *miR-200* family members, namely *miR-200a* (Fig. 4D), *miR-200c* (Fig. 4E) and *miR-429* (Fig. 4F), were all up-regulated in PRNRP cases compared to ccRCC cases and the latter two miRNAs were also up-regulated compared to PRCC cases but not significantly in the case of *miR-200a*. In the case of *miR-429*, levels of this miRNA were additionally significantly higher than control samples whereas this was not significant for either *miR-200a* or *mir-200c* levels. Similarly, levels of *miR-148a*, *miR-30c*, *miR-375* and *miR-203a* were significantly higher in PRNRP cases (Fig. 4G,H,I,J, respectively) than ccRCC, PRCC or controls, although not significantly so in the case of control levels of *miR-203a*. These data are summarised in Supplementary Table 11 (Appendix A).

We also looked at the expression of the predicted target genes of the differentially expressed miRNAs (i.e., *VEGFA*, *KRAS, ISCU, SERPINE1*, *CXCL8* and *STAT3* (Fig. 5). Levels of *VEGFA*, *KRAS* and *ISCU* were up-regulated in PRNRP cases compared to PRCC cases (Fig. 5A,B,C, respectively). Levels of *VEGFA* were significantly higher in ccRCC cases compared to PRNRP cases, whereas levels of *KRAS* and *ISCU* were down-regulated in ccRCC cases. In contrast,

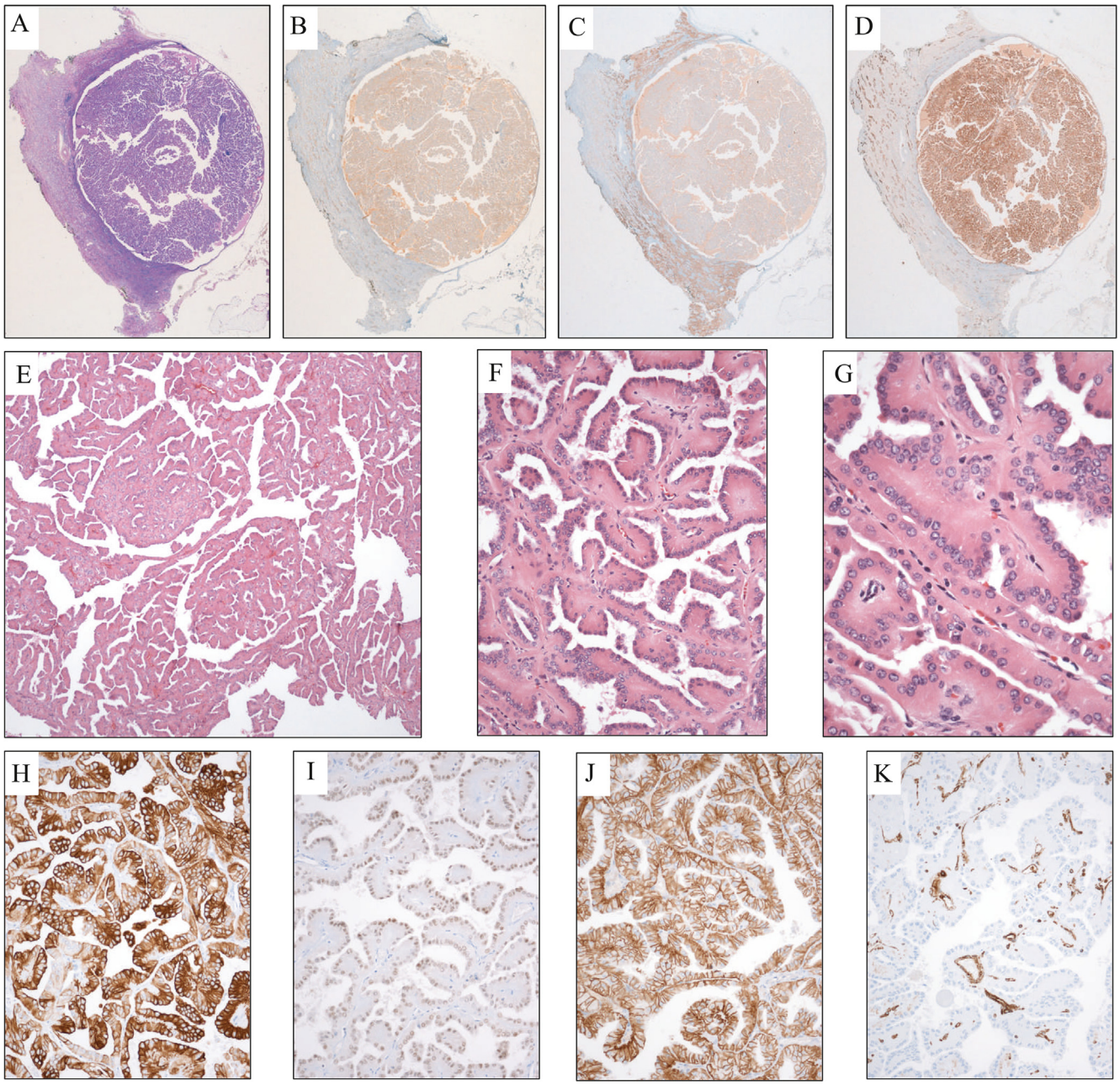

Fig. 1 Histological and immunohistochemical view of papillary renal neoplasm with reverse polarity (PRNRP) cases used in this study. Panoramic view of a representative example (Case 2): H&E (A), GATA-3 positivity (B), racemase positivity (C), L1CAM positivity with original magnification 1:1 (D). Histological details (Case 5) showing the characteristic papillary architecture, eosinophilic cellular appearance and reversal (anti-basal) polarity of tumour cell nuclei low power (E), medium power (F), high power (G). Immunohistochemical profile with CK7 positivity (cytoplasmic) (H), GATA-3 positivity (nuclear) (I), L1CAM positivity (membranous) (J), and vimentin negativity (K). Clinicopathological characteristics of PRNRP cases are in Table 1.

PRNRP levels of *SERPINE1, CXCL8* and *STAT3* (Fig. 5D,E,F, respectively) were down-regulated in PRNRP cases compared to control samples. These data are summarised in Supplementary Table 12 (Appendix A).

Gene set enrichment analysis (GSEA)

GSEA was conducted on gene microarray data to identify pathways significantly associated with differentially expressed genes between tumour types. The result of each analysis was illustrated by enrichment map using the Cytoscape software.[29] Two analyses were conducted, one comparing PRNRP vs PRCC cases (Fig. 6) and another one ccRCC vs PRNRP (Supplementary Fig. 5, Appendix A), respectively. Clusters containing gene sets represented by nodes were numbered based on their size. For the PRNRP vs PRCC comparison, all clusters were over-represented in PRNRP cases. The biggest cluster, *protein decay translation,* contained gene sets including cytoplasmic translation with a normalised enrichment score (NES)=2.83, protein targeting to ER (NES=4.45), protein targeting to membrane (NES=3.24) and nonsense-mediated decay (NMD) (NES=4.14). The third largest cluster *electron transport respiratory* comprised gene sets including mitochondrial ATP synthesis coupled electron transport (NES=3.88), NADH dehydrogenase complex assembly (NES=2.85) and

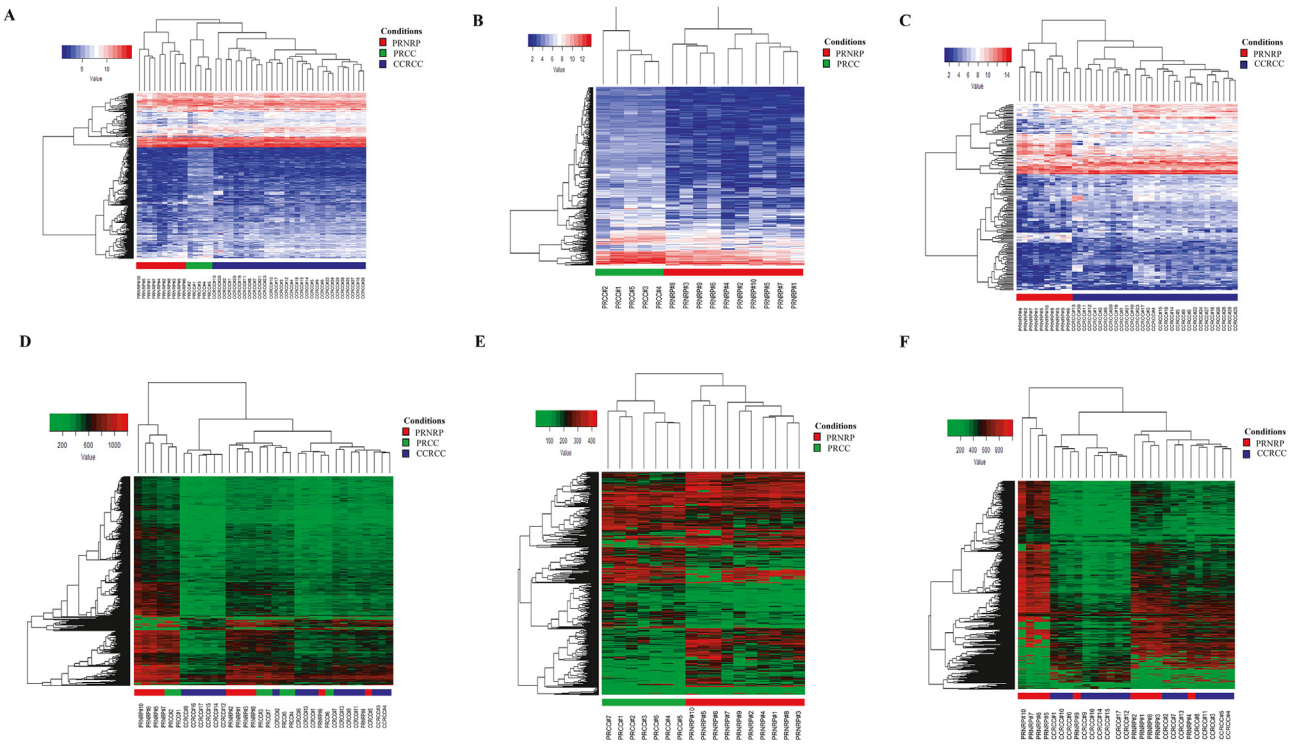

Fig. 2 The small non-coding RNA and gene expression profile of PRNRP is distinct from either PRCC or ccRCC cases. Unsupervised cluster analysis of mature miRNA expression data (average, $\log_2$ >2) (A) and cluster analysis of samples according to expression level of differentially expressed miRNA (>two-fold, p<0.05) between PRNRP and PRCC (B); and between PRNRP and ccRCC (C). Unsupervised cluster analysis of gene expression (D) and cluster analysis of samples according to expression level of differentially expressed genes (>two-fold, p<0.05) between PRNRP and PRCC (E); and between PRNRP and ccRCC (F). ccRCC, clear cell renal cell carcinoma; PRCC, papillary renal cell carcinoma; PRNRP, papillary renal neoplasm with reverse polarity.

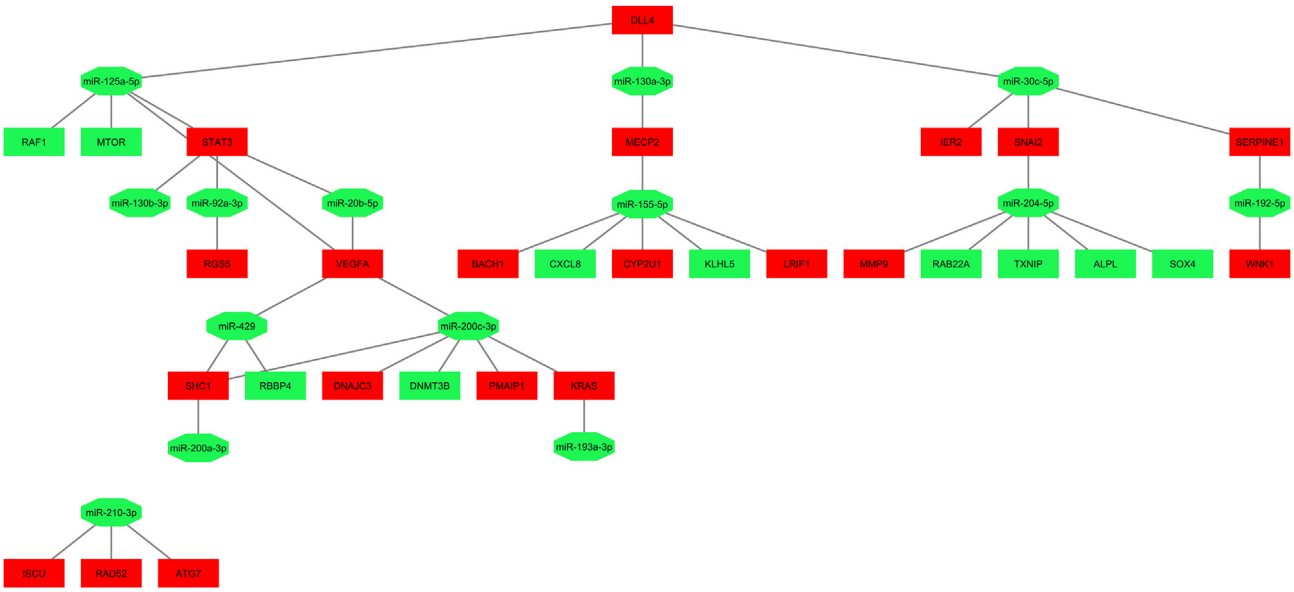

Fig. 3 miRNA:gene network analysis between PRNRP vs PRCC cases. Direct interaction between miRNA and gene differentially expressed between tumour type (one-fold difference, p<0.05) are illustrated. Square nodes represent target genes and octagonal nodes miRNAs, red colour denotes up-regulation and green down-regulation. A list of miRNA:gene interaction is in Table 2.

aerobic respiration (NES=3.45). Other relevant clusters included *acyl coA process*, *toll receptor cascade*, *transcript export nucleus*, *unsaturated fatty acid* and *phosphatidylinositol biosynthetic process* that comprise gene sets with NES between 2, 50 and 3.41. The complete list of clusters, corresponding gene sets, gene set size and normalised enrichment score (NES) illustrated in Fig. 6 are reported in Supplementary Table 13 (Appendix A).

For the ccRCC vs PRNRP comparison (Supplementary Fig. 5, Appendix A), the two biggest clusters by size *protein localisation endoplasmic* and *respiratory electron transport* were underrepresented in ccRCC compared to PRNRP with NES between −3.05 and −3.33. By comparing both enrichment maps, we observed that all of the 29 gene sets of the *protein localisation endoplasmic* cluster (ccRCC vs PRNRP; Supplementary Table 14, Appendix A) were also

Table 2 List of differentially expressed genes targeted by differentially expressed miRNAs following miRNA:gene network analysis between PRNRP vs PRCC cases[a]

miRNA	Target gene(s)
hsa-miR-125a-5p	*RAF1*, *MTOR*, *VEGFA**, *STAT3**, *DLL4*
hsa-miR-130a-3p	*DLL4*, *MECP2*
*hsa-miR-30c-5p**	*DLL4*, *IER2*, *SNAI2*, *SERPINE1**
hsa-miR-130b-3p	*STAT3**
hsa-miR-92a-3p	*STAT3**, *RGS5*
hsa-miR-20b-5p	*STAT3**, *VEGFA**
*hsa-miR-155-5p**	*BACH1*, *CXCL8**, *MECP2*, *CYP2U1*, *KLHL5*, *LRIF1*
hsa-miR-204-5p	*MMP9*, *RAB22A*, *SNAI2*, *TXNIP*, *ALPL*, *SOX4*
hsa-miR-192-5p	*SERPINE1**, *WNK1*
*hsa-miR-429**	*VEGFA**, *SHC1*, *RBBP4*
*hsa-miR-200c-3p**	*SHC1*, *DNAJC3*, *DNMT3B*, *PMAIP1*, *KRAS**
*hsa-miR-200a-3p**	*SHC1*
*hsa-miR-193a-3p**	*KRAS**
*hsa-miR-210-3p**	*ISCU**, *RAD52*, *ATG7*

PRCC, papillary renal cell carcinoma; PRNRP, papillary renal neoplasm with reverse polarity.
[a] Illustrated in Fig. 3.
* Indicates miRNAs and the respective target genes validated by qRT-PCR.

included in the *protein decay translation* cluster (PRNRP vs PRCC; Supplementary Table 13, Appendix A). Likewise, all of the 10 gene sets of the respiratory electron transport cluster (ccRCC vs PRNRP; Supplementary Table 14, Appendix A) were found in the *electron transport respiratory* cluster (PRNRP vs PRCC; Supplementary Table 13, Appendix A). In both enrichment maps, these gene sets were over-represented in PRNRP cases compared to either PRCC or ccRCC. The complete list of clusters, corresponding gene sets, gene set size and normalised enrichment score (NES) illustrated in Supplementary Fig. 5 (Appendix A) are reported in Supplementary Table 14 (Appendix A).

DISCUSSION

In 2019, PRNRP was defined as a new entity by Al-Obaidy *et al.* based on 18 cases that had previously been diagnosed as low-grade oncocytic papillary RCC.[10] Since this time, there have been over 20 studies that have reported ~150 PRNRP cases, all characterised by the presence of branching papillae with thin fibrovascular cores covered by cuboidal to columnar cells with granular eosinophilic cytoplasm and smooth luminal borders. The neoplastic cells had mostly regular nuclei with occasional nuclear clearing that were apically located (i.e., elevated from basal membrane), without conspicuous nucleoli.[10–12,16,18,19,21,22,33–36] At least some cases previously diagnosed as low-grade oncocytic tumours in the kidney probably corresponded to PRNRP cases.[37] Many of these studies reported positivity for CK7, GATA3 and L1CAM expression but were usually negative for vimentin expression.[10–12,16,18,19,21,22,33–36] Consistent with the literature we also found that our cases were positive for CK7, GATA3 and L1CAM but negative for vimentin expression. Indeed, the immunohistochemistry profile of both PRNRP and PRCC is similar except the former is positive for GATA-3 and L1CAM expression in addition to having frequent *KRAS* mutations, characteristics that can be used to differentiate between the two pathologies.[22] Sometimes, however, diagnosing PRNRP can be challenging as morphological overlaps can occur with other renal neoplasms [i.e., PRCC, CCPRCC, oncocytic PRCC (OPRCC) and MiT translocation RCC].[12,33] This can be important as PRNRP has an indolent clinical behaviour and misdiagnosis of a more aggressive renal malignancy could plausibly lead to over-treatment. In these cases, precise histomorphological examination, immunohistochemical staining, and *KRAS* mutation studies may help to establish a more accurate diagnosis.

In this study, we took a molecular approach to PRNRP characterisation by providing a comprehensive analysis of ncRNAs and gene expression in this pathology. Unsupervised cluster analysis of ncRNA expression revealed that the pattern of mature miRNA, pre miRNA and small nucleolar RNA and small Cajal body-specific RNA expression in PRNRP cases was distinct from either PRCC or ccRCC (Fig. 2A; Supplementary Fig. 1, Appendix A). In contrast, the pattern of gene expression did not cluster the PRNRP cases to the same extent as with ncRNA expression (Fig. 2D), suggesting that ncRNA expression rather than gene expression is important to the pathogenesis of PRNRP. To look in more detail at the role of ncRNA in this pathology we used network analysis to identify potential target genes of differentially expressed miRNAs. The fact that many of the miRNAs and their respective target genes were present in both comparisons (i.e., PRNRP vs PRCC and PRNRP vs ccRCC) suggests that not only miRNA expression differs between PRNRP and the other renal neoplasms but that these miRNAs regulate different genes, and therefore pathways, in PRNRP.

We validated selected miRNAs and target genes in an extended cohort of 10 PRNRP, 20 ccRCC and 20 PRCC cases along with 22 healthy control samples by qRT-PCR. We observed that the tumour-promoting miRNA *miR-155* showed similar levels of expression than normal tissues, unlike in ccRCC and PRCC tissues where it was significantly up-regulated. In general, *miR-155* is up-regulated in most solid tumours and its target genes are involved in tumourigenesis, DNA damage repair and inflammation.[38,39] Similarly, we observed that *miR-210* was up-regulated in ccRCC and PRCC compared to control tissue but not in the case of PRNRP. This miRNA is up-regulated by hypoxia through direct transcriptional regulation by hypoxia-inducible transcription factors (HIFs),[40–43] and ccRCC shows constitutive up-regulation of *miR*-210 that is independent of oxygen status through deregulation of the VHL–HIF pathway.[44]

Interestingly, we found that all members of the *miR-200* family (i.e., *miR-200a*, *miR-200c* and *miR-429*), were over-expressed in PRNRP cases compared to ccRCC, PRCC or control samples (Fig. 4D,E, 4F). In contrast other renal carcinoma types including ccRCC and PRCC are characterised by down-regulation of these miRNAs compared to normal renal tissue.[44–46] These miRNAs regulate epithelial mesenchymal transition (EMT),[47] a hallmark of tumour aggressiveness and metastatic progression.[48,49] Interestingly, we also previously found up-regulation of these miRNAs in clear cell PRCC (CCPRCC)[24] and tubulocystic RCC (TC-RCC),[23]

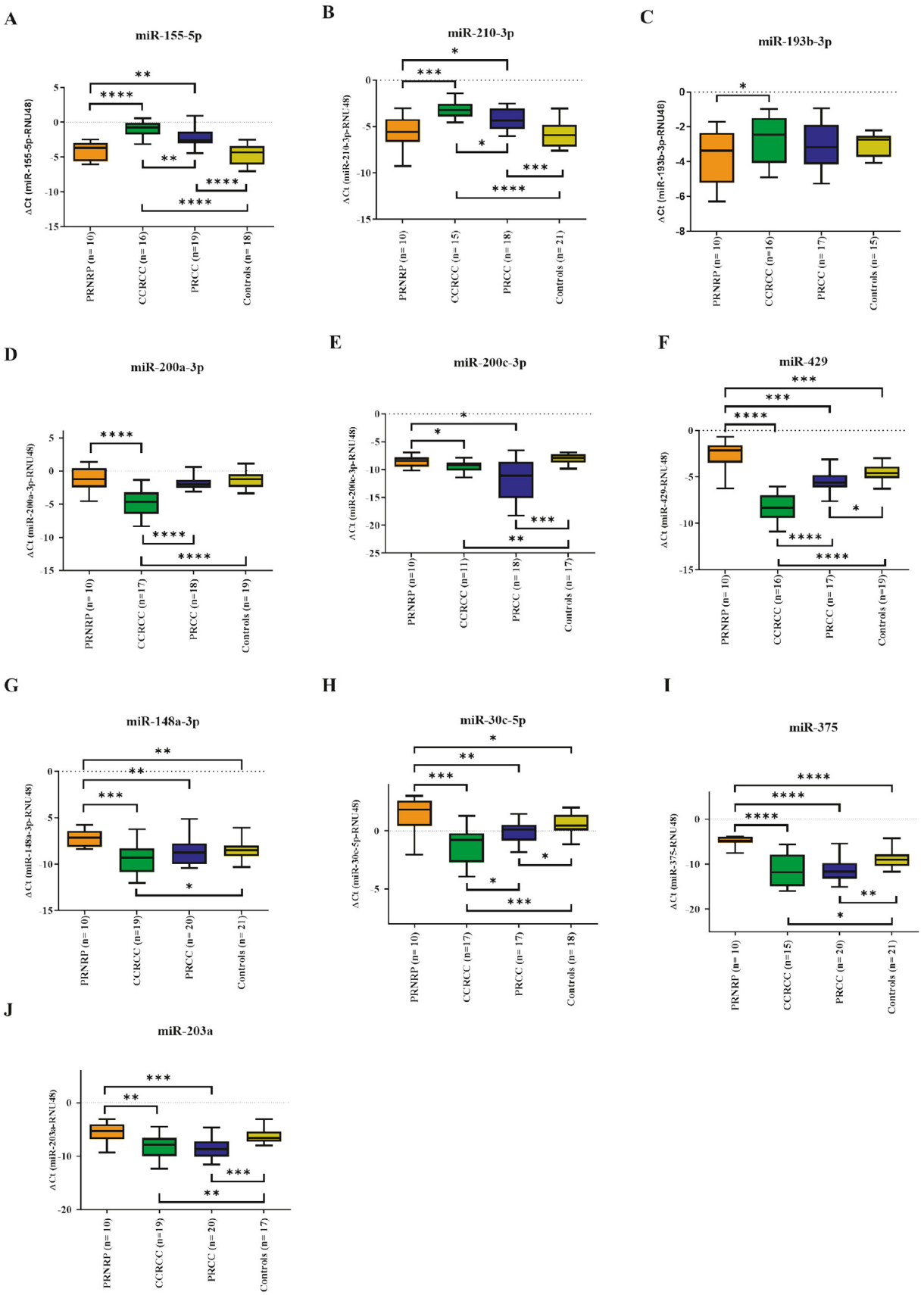

Fig. 4 Expression levels of miRNAs in validation cohort measured by quantitative RT-PCR. *miR-155-5p* (A), *miR-210-3p* (B), *miR-193b-3p* (C), *miR-200a-3p* (D), *miR-200c-3p* (E), *miR-429* (F), *miR-148a-3p* (G), *miR-30c-5p* (H), *miR-375* (I), and *miR-203a* (J) levels in papillary renal neoplasm with reverse polarity (PRNRP), clear cell renal cell carcinoma (ccRCC), papillary renal cell carcinoma (PRCC) and controls. A summary list of miRNAs differentially expressed in PRNRP compared with other renal neoplasms is reported in Supplementary Table 11 (Appendix A). Nondetectable samples were excluded from the analysis. *p* values were calculated by Mann–Whitney independent t-test. *$p<0.05$, **$p<0.01$, ***$p<0.001$, and ****$p<0.0001$.

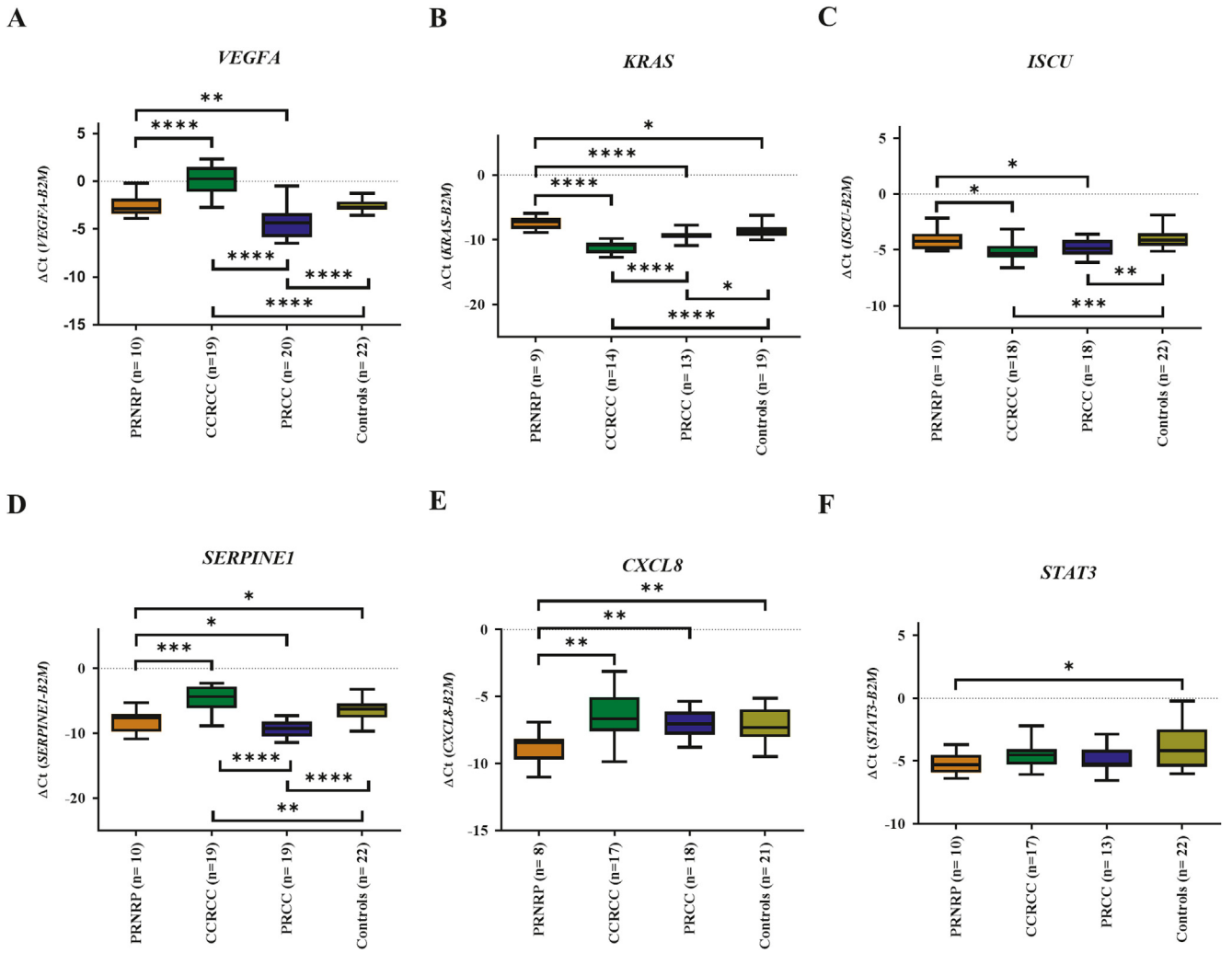

Fig. 5 Expression levels of genes in validation cohort measured by quantitative RT-PCR. *VEGFA* (A), *KRAS* (B), *ISCU* (C), *SERPINE1* (D), *CXCL8* (E), *STAT3* (F), levels in papillary renal neoplasm with reverse polarity (PRNRP), clear cell renal cell carcinoma (ccRCC), papillary renal cell carcinoma (PRCC) and controls. A summary list of genes differentially expressed in PRNRP compared with other renal neoplasms is reported in Supplementary Table 12 (Appendix A). Nondetectable samples were excluded from the analysis. *p* values were calculated by Mann–Whitney independent t-test. *$p<0.05$, **$p<0.01$, ***$p<0.001$, and ****$p<0.0001$.

both of which are indolent renal neoplasms that share features of PRCC. Similarly, we found that *miR-30c* was up-regulated in PRNRP cases. This miRNA acts as a tumour suppressor miRNA that can inhibit cell proliferation, invasion, and metastasis in prostate cancer via inhibition of the KRAS-MAPK signalling axis.[50] We also observed that *miR-148a*, another regulator of EMT,[47] was also over-expressed in PRNRP compared to other renal cancer types. Interestingly, *miR-148a* has been found to target *SERPINE1*, inhibiting EMT development in colon adenocarcinoma,[51] consistent with the vimentin negativity observed with PRNRP.

In addition to miRNAs, we also investigated the expression of their respective target genes. We observed an up-regulation of *KRAS*, an oncogene that is frequently mutated in PRNRP, most commonly manifest as missense mutations in exon 2 codon 12 (pG12X), which was present in seven of 10 of the cases included in the present study, corresponding to the 60–70% of cases described in the literature.[22,52,53] We analysed the miRNA and gene expression data to see if there were any differences between *KRAS*-mutated and *KRAS*-non-mutated PRNRP cases but did not observe any significant differences. This could be due to the low number of *KRAS*-non-mutated PRNRP cases (n=3). Another intriguing feature of *KRAS* in PRNRP is that although the presence of nonsense mutation in the cases makes this protein non-functional in PRNRP, we still observed that *KRAS* levels were up-regulated (including *KRAS*-non-mutated PRNRP cases). Interestingly both PRCC and ccRCC, which rarely harbour *KRAS* mutations, are characterised by a down-regulation of *KRAS*.[54] A possible explanation for this apparent phenomenon is that *miR-193b,* which targets *KRAS,* was observed to be down-regulated in PRNRP compared to control cases so may explain the redundant over-expression of *KRAS*. Indeed, it has previously been reported that down-regulation of *miR-193b* is coupled with *KRAS* over-expression in pancreatic ductal adenocarcinoma and was found to contribute to tumour cell growth through the modulation of AKT and ERK pathways.[55]

In contrast to *KRAS* we observed that *CXCL8* was down-regulated in PRNRP compared to control and other renal

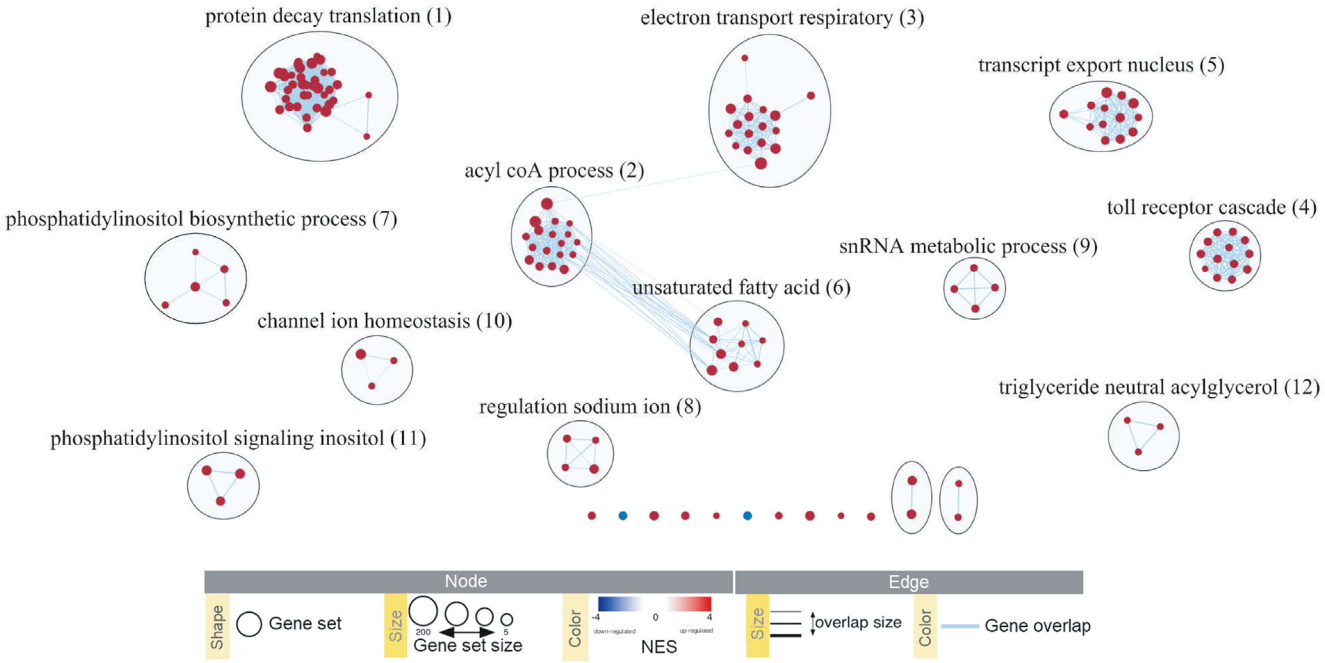

Fig. 6 Pathways differentially expressed between papillary renal neoplasm with reverse polarity (PRNRP) and papillary renal cell carcinoma (PRCC) cases. Gene Set Enrichment Analysis (GSEA) showed different activation of metabolic pathways between renal neoplasms. Node size corresponds to the number of genes comprising the gene set. The normalised enrichment scores (NES) for the gene sets are represented by the node's colour (red indicates up-regulation, blue represents down-regulation). To identify redundancies between gene sets, the nodes are connected with edges if their contents overlap by more than 50%. Thickness of the edge corresponds to the size of the overlap. $p<0.01$, FDR$\leq$0.15.

neoplasms. *CXCL8* (IL-8) is targeted by *miR-155,*[56] and overexpression of this miRNA has been demonstrated to decrease levels of IL-37 protein and to enhance the production of CXCL8.[57] Furthermore, IL-8(*CXCL8*)/CXCR1 has been found to be involved in many molecular processes in ccRCC including proliferation, migration, invasion, sphere formation and self-renewal capabilities.[58] We also validated *ISCU*, a target of *miR-210,* which is a component of the iron–sulfur (Fe–S) cluster scaffold and is involved in electron transport and oxidation–reduction reactions.[59,60] Higher levels of *ISCU* were observed in PRNRP and control samples compared to ccRCC and PRCC cases. In contrast, levels of *VEGFA*, a target of *HIF1A*, were down-regulated compared to ccRCC and PRCC. A possible explanation is that *miR-429* targets *VEGFA,*[61] and we found that it was up-regulated in PRNRP but down-regulated in both ccRCC and PRCC cases (compared to healthy controls). We observed that *SERPINE1,* a target for *miR-30c* which was up-regulated in PRNRP cases, was also down-regulated compared to ccRCC cases. *SERPINE1* is part of the serine protein kinase inhibitor family involved in the fibrinolysis process,[62] which has been reported as a pro-tumourigenesis factor and a member of EMT pathway.[63,64] In addition, we validated *STAT3*, a target of *miR-148a*,[65] which was down-regulated compared to healthy controls although no difference of expression was observed between PRNRP cases and ccRCC or PRCC cases.

In order to further examine the potential role of the identified miRNA:target genes we carried out GSEA on the target genes to determine gene sets over-represented in PRNRP compared to PRCC (Fig. 6) and ccRCC (Supplementary Fig. 5, Appendix A), respectively. We observed that pathways involved in normal cellular respiration were overexpressed in PRNRP cases compared to either PRCC or ccRCC cases. This finding is consistent with a recent study that used GSEA on PRCC and healthy kidney tissues[66] and reported a significant under-representation of oxidative phosphorylation pathways in PRCC.

Additionally, we found that gene sets involved in RNA processing and nonsense-mediated RNA decay (NMD) were enriched in PRNRP compared to other renal neoplasms. NMD is a conserved mRNA surveillance pathway that cells use to ensure the quality of transcripts and to fine-tune transcript abundance,[67] and there is clear evidence of tumours exploiting NDM,[68–70] either as a tumour-suppressive pathway or tumour promoting, depending on the genetic evolutionary history of the tumour.[67,69,71]

Our analysis of miRNA expression in PRNRP cases suggests that there are no commonly deregulated miRNAs in different types of RCC tumours, consistent with what has previously been reported.[72] However, since their expression pattern is distinct from normal tissues and other renal neoplasms, we suggest that miRNAs such as *miR-429*, *miR-148a*, *miR-30c* and *miR-375* could be used as biomarkers to identify PRNRP cases or to confirm histopathological findings.

Furthermore, our results suggest that at the level of ncRNA and gene expression, at least, PRNRP represents a distinct molecular entity and adds to the mounting evidence that this renal neoplasm should be formally considered a distinct entity from PRCC.

Acknowledgements: We dedicate this article to the late Dr Ondrej Hes who tragically died during the drafting of this manuscript.

Conflicts of interest and sources of funding: CHL and his research are supported by grants from the IKERBASQUE Basque Foundation for Science, the Starmer-Smith Memorial Fund, the Instituto de Salud Carlos III (ISCIII), Spain, through the project PI23/00907, and co-funded by the European Union, Departamento de Sanidad of Gobierno Vasco, Spain, through the project 2023333023, and Departamento de Industria of Gobierno Vasco, Spain, through the projects KK-2022/00008 and KK-2023/00001. The authors state that there are no conflicts of interest to disclose.

APPENDIX A. SUPPLEMENTARY DATA

Supplementary data to this article can be found online at https://doi.org/10.1016/j.pathol.2023.11.013.

Address for correspondence: Dr Charles H. Lawrie, Biodonostia Research Institute, Paseo Doctor Begiristain, San Sebastián 20014, Spain. E-mail: charles.lawrie@biodonostia.org

References

1. Siegel RL, Miller KD, Fuchs HE, Jemal A. Cancer statistics, 2022. *CA Cancer J Clin* 2022; 72: 7–33.
2. Souza DLB, Bernal MM. Incidence, prevalence and mortality of kidney cancer in Spain: estimates and projections for the 1998–2022 period. *Actas Urológicas Españolas (English Ed)* 2012; 36: 521–6.
3. Srigley JR, Delahunt B, Eble JN, *et al*. The International Society of Urological Pathology (ISUP) Vancouver Classification of Renal Neoplasia. *Am J Surg Pathol* 2013; 37: 1469–89.
4. Moch H, Cubilla AL, Humphrey PA, Reuter VE, Ulbright TM. The 2016 WHO Classification of Tumours of the Urinary System and Male Genital Organs–Part A: renal, penile, and testicular tumours. *Eur Urol* 2016; 70: 93–105.
5. Tickoo SK, Reuter VE. Differential diagnosis of renal tumors with papillary architecture. *Adv Anat Pathol* 2011; 18: 120–32.
6. López JI. Renal tumors with clear cells. A review. *Pathol Res Pract* 2013; 209: 137–46.
7. Lopez-Beltran A, Scarpelli M, Montironi R, Kirkali Z. 2004 WHO classification of the renal tumors of the adults. *Eur Urol* 2006; 49: 798–805.
8. Nagashima Y, Inayama Y, Kato Y, *et al*. Pathological and molecular biological aspects of the renal epithelial neoplasms, up-to-date. *Pathol Int* 2004; 54: 377–86.
9. Moch H, Amin MB, Berney DM, *et al*. The 2022 World Health Organization Classification of Tumours of the Urinary System and Male Genital Organs–Part A: renal, penile, and testicular tumours. *Eur Urol* 2022; 82: 458–68.
10. Al-Obaidy KI, Eble JN, Cheng L, *et al*. Papillary renal neoplasm with reverse polarity: a morphologic, immunohistochemical, and molecular study. *Am J Surg Pathol* 2019; 43: 1099–111.
11. Wei S, Kutikov A, Patchefsky AS, *et al*. Papillary renal neoplasm with reverse polarity is often cystic: report of 7 cases and review of 93 cases in the literature. *Am J Surg Pathol* 2022; 46: 336–43.
12. Kim SS, Cho YM, Kim GH, *et al*. Recurrent KRAS mutations identified in papillary renal neoplasm with reverse polarity—a comparative study with papillary renal cell carcinoma. *Mod Pathol* 2020; 33: 690–9.
13. Lee HJ, Shin DH, Park JY, *et al*. Unilateral synchronous papillary renal neoplasm with reverse polarity and clear cell renal cell carcinoma: a case report with KRAS and PIK3CA mutations. *Diagn Pathol* 2020; 15: 123.
14. Tong K, Zhu W, Fu H, *et al*. Frequent KRAS mutations in oncocytic papillary renal neoplasm with inverted nuclei. *Histopathology* 2020; 76: 1071–83.
15. Zhou L, Xu J, Wang S, *et al*. Papillary renal neoplasm with reverse polarity: a clinicopathologic study of 7 cases. *Int J Surg Pathol* 2020; 28: 728–34.
16. Kiyozawa D, Kohashi K, Takamatsu D, *et al*. Morphological, immunohistochemical, and genomic analyses of papillary renal neoplasm with reverse polarity. *Hum Pathol* 2021; 112: 48–58.
17. Pivovarcikova K, Grossmann P, Hajkova V, *et al*. Renal cell carcinomas with tubulopapillary architecture and oncocytic cells: molecular analysis of 39 difficult tumors to classify. *Ann Diagn Pathol* 2021; 52: 151734.
18. Chang HY, Hang JF, Wu CY, *et al*. Clinicopathological and molecular characterisation of papillary renal neoplasm with reverse polarity and its renal papillary adenoma analogue. *Histopathology* 2021; 78: 1019–31.
19. Nova-Camacho LM, Martin-Arruti M, Ruiz Díaz I, Panizo-Santos Á. Papillary renal neoplasm with reverse polarity. *Arch Pathol Lab Med* 2022; 147: 692–700.
20. Al-Obaidy KI, Eble JN, Nassiri M, *et al*. Recurrent KRAS mutations in papillary renal neoplasm with reverse polarity. *Mod Pathol* 2020; 33: 1157–64.
21. Yang T, Kang E, Zhang L, *et al*. Papillary renal neoplasm with reverse polarity may be a novel renal cell tumor entity with low malignant potential. *Diagn Pathol* 2022; 17: 66.
22. Kim B, Lee S, Moon KC. Papillary renal neoplasm with reverse polarity: a clinicopathologic study of 43 cases with a focus on the expression of KRAS signalling pathway downstream effectors. *Hum Pathol* 2023; 142: 1–6.
23. Lawrie CH, Armesto M, Fernandez-Mercado M, *et al*. Noncoding RNA expression and targeted next-generation sequencing distinguish tubulocystic renal cell carcinoma (TC-RCC) from other renal neoplasms. *J Mol Diagn* 2018; 20: 34–45.
24. Lawrie CH, Larrea E, Larrinaga G, *et al*. Targeted next-generation sequencing and non-coding RNA expression analysis of clear cell papillary renal cell carcinoma suggests distinct pathological mechanisms from other renal tumour subtypes. *J Pathol* 2014; 232: 32–42.
25. R Core Team. *R: A Language and Environment for Statistical Computing*. Vienna: R Foundation for Statistical Computing, 2022.
26. Wickham H. *ggplot2: Elegant Graphics for Data Analysis*. Springer, 2009.
27. Armesto M, Marquez M, Arestin M, *et al*. Integrated mRNA and miRNA transcriptomic analyses reveals divergent mechanisms of sunitinib resistance in clear cell renal cell carcinoma (ccRCC). *Cancers (Basel)* 2021; 13: 4401.
28. Hsu S da, Lin FM, Wu WY, *et al*. miRTarBase: a database curates experimentally validated microRNA–target interactions. *Nucleic Acids Res* 2011; 39: D163–9.
29. Smoot ME, Ono K, Ruscheinski J, Wang PL, Ideker T. Cytoscape 2.8: new features for data integration and network visualization. *Bioinformatics* 2011; 27: 431–2.
30. Subramanian A, Tamayo P, Mootha VK, *et al*. Gene set enrichment analysis: a knowledge-based approach for interpreting genome-wide expression profiles. *Proc Natl Acad Sci USA* 2005; 102: 15545–50.
31. Reimand J, Isserlin R, Voisin V, *et al*. Pathway enrichment analysis and visualization of omics data using g:Profiler, GSEA, Cytoscape and EnrichmentMap. *Nat Protoc* 2019; 14: 482–517.
32. Lawrie CH, Ballabio E, Dyar OJ, *et al*. MicroRNA expression in chronic lymphocytic leukaemia. *Br J Haematol* 2009; 147: 398–402.
33. Wang T, Ding X, Huang X, *et al*. Papillary renal neoplasm with reverse polarity—a comparative study with CCPRCC, OPRCC, and PRCC1. *Hum Pathol* 2022; 129: 60–70.
34. Conde-Ferreirós M, Domínguez-de Dios J, Juaneda-Magdalena L, *et al*. Papillary renal cell neoplasm with reverse polarity: a new subtype of renal tumour with favorable prognosis. *Actas Urol Esp* 2022; 46: 600–5.
35. Shen M, Yin X, Bai Y, *et al*. Papillary renal neoplasm with reverse polarity: a clinicopathological and molecular genetic characterization of 16 cases with expanding the morphologic spectrum and further support for a novel entity. *Front Oncol* 2022; 12: 930296.
36. Liu Y, Zhang H, Li X, *et al*. Papillary renal neoplasm with reverse polarity with a favorable prognosis should be separated from papillary renal cell carcinoma. *Hum Pathol* 2022; 127: 78–85.
37. Samaratunga H, Egevad L, Thunders M, *et al*. LOT and HOT or not. The proliferation of clinically insignificant and poorly characterised types of renal neoplasia. *Pathology* 2022; 54: 842–7.
38. Bayraktar R, van Roosbroeck K. miR-155 in cancer drug resistance and as target for miRNA-based therapeutics. *Cancer Metastasis Rev* 2018; 37: 33–44.
39. Faraoni I, Antonetti FR, Cardone J, Bonmassar E. miR-155 gene: a typical multifunctional microRNA. *Biochim Biophys Acta* 2009; 1792: 497–505.
40. Kulshreshtha R, Ferracin M, Wojcik SE, *et al*. A microRNA signature of hypoxia. *Mol Cell Biol* 2007; 27: 1859–67.
41. Fasanaro P, D'Alessandra Y, di Stefano V, *et al*. MicroRNA-210 modulates endothelial cell response to hypoxia and inhibits the receptor tyrosine kinase ligand Ephrin-A3. *J Biol Chem* 2008; 283: 15878–83.
42. Crosby ME, Kulshreshtha R, Ivan M, Glazer PM. MicroRNA regulation of DNA repair gene expression in hypoxic stress. *Cancer Res* 2009; 69: 1221–30.

43. Camps C, Buffa FM, Colella S, *et al*. hsa-miR-210 is induced by hypoxia and is an independent prognostic factor in breast cancer. *Clin Cancer Res* 2008; 14: 1340–8.
44. Nakada C, Matsuura K, Tsukamoto Y, *et al*. Genome-wide microRNA expression profiling in renal cell carcinoma: significant down-regulation of miR-141 and miR-200c. *J Pathol* 2008; 216: 418–27.
45. Al-Ali BM, Ress AL, Gerber A, Pichler M. MicroRNAs in renal cell carcinoma: implications for pathogenesis, diagnosis, prognosis and therapy. *Anticancer Res* 2012; 32: 3727–32.
46. Duns G, van den Berg A, van Dijk MCRF, *et al*. The entire miR-200 seed family is strongly deregulated in clear cell renal cell cancer compared to the proximal tubular epithelial cells of the kidney. *Genes Chromosomes Cancer* 2013; 52: 165–73.
47. Korpal M, Kang Y. The emerging role of miR-200 family of MicroRNAs in epithelial-mesenchymal transition and cancer metastasis. *RNA Biol* 2008; 5: 115–9.
48. Sciacovelli M, Gonçalves E, Johnson TI, *et al*. Fumarate is an epigenetic modifier that elicits epithelial-to-mesenchymal transition. *Nature* 2016; 537: 544.
49. Letouzé E, Martinelli C, Loriot C, *et al*. SDH mutations establish a hypermethylator phenotype in paraganglioma. *Cancer Cell* 2013; 23: 739–52.
50. Ling XH, Han ZD, Xia D, *et al*. MicroRNA-30c serves as an independent biochemical recurrence predictor and potential tumor suppressor for prostate cancer. *Mol Biol Rep* 2014; 41: 2779–88.
51. Hu B, Chen Z, Wang X, Chen F, Song Z, Cao C. MicroRNA-148a-3p directly targets SERPINE1 to suppress EMT-mediated colon adenocarcinoma progression. *Cancer Manag Res* 2021; 13: 6349.
52. Cox AD, Fesik SW, Kimmelman AC, Luo J, Der CJ. Drugging the undruggable RAS: mission possible? *Nat Rev Drug Discov* 2014; 13: 828–51.
53. Prior IA, Lewis PD, Mattos C. A comprehensive survey of Ras mutations in cancer. *Cancer Res* 2012; 72: 2457.
54. Kumar A, Kumari N, Gupta V, Prasad R. Renal cell carcinoma: molecular aspects. *Indian J Clin Biochem* 2018; 33: 246–54.
55. Jin X, Sun Y, Yang H, *et al*. Deregulation of the MiR-193b-KRAS axis contributes to impaired cell growth in pancreatic cancer. *PLoS One* 2015; 10: e0125515.
56. Gao Y, Ma X, Yao Y, *et al*. miR-155 regulates the proliferation and invasion of clear cell renal cell carcinoma cells by targeting E2F2. *Oncotarget* 2016; 7: 20324.
57. Pashangzadeh S, Motallebnezhad M, Vafashoar F, Khalvandi A, Mojtabavi N. Implications the role of miR-155 in the pathogenesis of autoimmune diseases. *Front Immunol* 2021; 12: 1645.
58. Corrò C, Healy ME, Engler S, *et al*. IL-8 and CXCR1 expression is associated with cancer stem cell-like properties of clear cell renal cancer. *J Pathol* 2019; 248: 377–89.
59. Tong WH, Rouault T. Distinct iron-sulfur cluster assembly complexes exist in the cytosol and mitochondria of human cells. *EMBO J* 2000; 19: 5692–700.
60. Rouault TA, Maio N. Biogenesis and functions of mammalian iron-sulfur proteins in the regulation of iron homeostasis and pivotal metabolic pathways. *J Biol Chem* 2017; 292: 12744–53.
61. Chen D, Li Y, Li Y, *et al*. Tumor suppressive microRNA-429 regulates cellular function by targeting VEGF in clear cell renal cell carcinoma. *Mol Med Rep* 2016; 13: 1361–6.
62. Binder BR, Christ G, Gruber F, *et al*. Plasminogen activator inhibitor 1: physiological and pathophysiological roles. *News Physiol Sci* 2002; 17: 56–61.
63. Placencio VR, DeClerck YA. Plasminogen activator inhibitor-1 in cancer: rationale and insight for future therapeutic testing. *Cancer Res* 2015; 75: 2969–74.
64. Rokavec M, Öner MG, Li H, *et al*. IL-6R/STAT3/miR-34a feedback loop promotes EMT-mediated colorectal cancer invasion and metastasis. *J Clin Invest* 2014; 124: 1853–67.
65. Zhang L, Li J, Wang Q, *et al*. The relationship between microRNAs and the STAT3-related signaling pathway in cancer. *Tumor Biol* 2017; 39: 1–11.
66. Meierhofer D, Al Ahmad A, Paffrath V, *et al*. Papillary renal cell carcinomas rewire glutathione metabolism and are deficient in both anabolic glucose synthesis and oxidative phosphorylation. *Cancers (Basel)* 2019; 11: 1298.
67. Popp MW, Maquat LE. Nonsense-mediated mRNA decay and cancer. *Curr Opin Genet Dev* 2018; 48: 44–50.
68. Tan K, Stupack DG, Wilkinson MF. Nonsense-mediated RNA decay: an emerging modulator of malignancy. *Nat Rev Cancer* 2022; 22: 437–51.
69. Nogueira G, Fernandes R, García-Moreno JF, Romão L. Nonsense-mediated RNA decay and its bipolar function in cancer. *Mol Cancer* 2021; 20: 72.
70. Nagar P, Islam MR, Rahman MA. Nonsense-mediated mRNA decay as a mediator of tumorigenesis. *Genes (Basel)* 2023; 14: 357.
71. Fernandes R, Nogueira G, da Costa PJ, Pinto F, Romão L. Nonsense-mediated mRNA decay in development, stress and cancer. *Adv Exp Med Biol* 2019; 1157: 41–83.
72. Kajdasz A, Majer W, Kluzek K, *et al*. Identification of RCC subtype-specific microRNAs-meta-analysis of high-throughput RCC tumor microRNA expression data. *Cancers (Basel)* 2021; 13: 1–21.